Received: 27 June 2023 | Revised: 29 August 2023 | Accepted: 17 September 2023

DOI: 10.1002/trc2.12429

Alzheimer's & Dementia
Translational Research & Clinical Interventions

RESEARCH ARTICLE

SHIP1 therapeutic target enablement: Identification and evaluation of inhibitors for the treatment of late-onset Alzheimer's disease

Cynthia D. Jesudason[1] | Emily R. Mason[2] | Shaoyou Chu[2] | Adrian L. Oblak[2,3] | June Javens-Wolfe[4] | Mustapha Moussaif[4] | Greg Durst[1] | Philip Hipskind[1] | Daniel E. Beck[5] | Jiajun Dong[6] | Ovini Amarasinghe[6] | Zhong-Yin Zhang[5,6] | Adam K. Hamdani[7] | Kratika Singhal[7] | Andrew D. Mesecar[7] | Sarah Souza[8] | Marlene Jacobson[8] | Jerry Di Salvo[8] | Disha M. Soni[2] | Murugesh Kandasamy[2] | Andrea R. Masters[2] | Sara K Quinney[2] | Suzanne Doolen[9] | Hasi Huhe[9] | Stacey J. Sukoff Rizzo[9] | Bruce T. Lamb[2,3] | Alan D. Palkowitz[2,4] | Timothy I. Richardson[2,3,4]

[1]Lgenia, Fortville, Indiana, USA

[2]Indiana University School of Medicine, Indianapolis, Indiana, USA

[3]Stark Neurosciences Research Institute, Indiana University School of Medicine, Indianapolis, Indiana, USA

[4]Indiana Biosciences Research Institute, Indianapolis, Indiana, USA

[5]Institute for Drug Discovery, Purdue University, West Lafayette, Indiana, USA

[6]Department of Medicinal Chemistry and Molecular Pharmacology, Purdue University, West Lafayette, Indiana, USA

[7]Department of Biochemistry, Purdue University, West Lafayette, Indiana, USA

[8]Evotec, Princeton, New Jersey, USA

[9]University of Pittsburgh School of Medicine, Pittsburgh, Pennsylvania, USA

Correspondence
Timothy I. Richardson, Biotechnology Research & Training Center, 1345 W 16th St, Indianapolis, IN 46202, USA.
Email: timorich@iu.edu

Funding information
National Institutes of Health, Grant/Award Numbers: U54 AG065181, P30 CA082709

Abstract

INTRODUCTION: The risk of developing Alzheimer's disease is associated with genes involved in microglial function. Inositol polyphosphate-5-phosphatase (*INPP5D*), which encodes Src homology 2 (SH2) domain–containing inositol polyphosphate 5-phosphatase 1 (SHIP1), is a risk gene expressed in microglia. Because SHIP1 binds receptor immunoreceptor tyrosine-based inhibitory motifs (ITIMs), competes with kinases, and converts PI(3,4,5)P_3 to PI(3,4)P_2, it is a negative regulator of microglia function. Validated inhibitors are needed to evaluate SHIP1 as a potential therapeutic target.

METHODS: We identified inhibitors and screened the enzymatic domain of SHIP1. A protein construct containing two domains was used to evaluate enzyme inhibitor

potency and selectivity versus SHIP2. Inhibitors were tested against a construct containing all ordered domains of the human and mouse proteins. A cellular thermal shift assay (CETSA) provided evidence of target engagement in cells. Phospho-AKT levels provided further evidence of on-target pharmacology. A high-content imaging assay was used to study the pharmacology of SHIP1 inhibition while monitoring cell health. Physicochemical and absorption, distribution, metabolism, and excretion (ADME) properties were evaluated to select a compound suitable for in vivo studies.

RESULTS: SHIP1 inhibitors displayed a remarkable array of activities and cellular pharmacology. Inhibitory potency was dependent on the protein construct used to assess enzymatic activity. Some inhibitors failed to engage the target in cells. Inhibitors that were active in the CETSA consistently destabilized the protein and reduced pAKT levels. Many SHIP1 inhibitors were cytotoxic either at high concentration due to cell stress or they potently induced cell death depending on the compound and cell type. One compound activated microglia, inducing phagocytosis at concentrations that did not result in significant cell death. A pharmacokinetic study demonstrated brain exposures in mice upon oral administration.

DISCUSSION: 3-((2,4-Dichlorobenzyl)oxy)-5-(1-(piperidin-4-yl)-1H-pyrazol-4-yl) pyridine activated primary mouse microglia and demonstrated exposures in mouse brain upon oral dosing. Although this compound is our recommended chemical probe for investigating the pharmacology of SHIP1 inhibition at this time, further optimization is required for clinical studies.

KEYWORDS

cellular thermal shift assay (CETSA), INPP5D, pharmacokinetics, phenotypic high-content imaging assay, SHIP1, SHIP1 inhibitors

Highlights

- Cellular thermal shift assay (CETSA) and signaling (pAKT) assays were developed to provide evidence of src homology 2 (SH2) domain-contaning inositol phosphatase 1 (SHIP1) target engagement and on-target activity in cellular assays.
- A phenotypic high-content imaging assay with simultaneous measures of phagocytosis, cell number, and nuclear intensity was developed to explore cellular pharmacology and monitor cell health.
- SHIP1 inhibitors demonstrate a wide range of activity and cellular pharmacology, and many reported inhibitors are cytotoxic.
- The chemical probe 3-((2,4-dichlorobenzyl)oxy)−5-(1-(piperidin-4-yl)−1H-pyrazol-4-yl) pyridine is recommended to explore SHIP1 pharmacology.

1 | BACKGROUND

Alzheimer's disease (AD) is a progressive neurodegenerative disorder that is characterized by the accumulation of abnormal protein aggregates, including amyloid beta (Aβ) plaques and tau tangles, in the brain. Gradual neurodegeneration leads to cognitive decline, memory loss, and behavioral changes. Specific triggers and mechanisms are not yet fully understood; however, they likely result from a complex interplay of genetics, environment, and lifestyle. Genome-wide association studies (GWAS), whole genome sequencing, and gene-expression network analyses comparing normal aged brain to samples from patients with late-onset Alzheimer's disease (LOAD) have identified protective and risk genes involved in microglia function and neuroinflammation.[1–4] Target selection and validation based on these studies remains a challenge. It is often unclear if a successful therapeutic intervention would require a target to be upregulated

or downregulated and the timing of such interventions remain unclear.

The TaRget Enablement to Accelerate Therapy Development for Alzheimer's Disease (TREAT-AD) centers were established to provide high-quality research tools and technologies to validate and advance the next generation of drug targets for AD.[5] Data, methods, and computational and experimental tools are being openly disseminated and free-of-charge to the broader research community for use in drug discovery and in research to better understand the complex biology of AD. Resources are made available in a Target Enablement Package (TEP) at the AD Knowledge Portal (https://adknowledgeportal.synapse.org/Explore/Target%20Enabling%20Resources). Here the IUSM-Purdue TREAT-AD Center is reporting a chemical probe TEP with methods and experimental tools that we hope will catalyze and support further investigation into SHIP1 as a target for the treatment of AD.[6]

The inositol polyphosphate-5-phosphatase (*INPP5D*) gene has been identified as a risk gene for AD by a meta-analysis of four large genome-wide association studies (GWAS),[7] and has been nominated as a therapeutic target by three teams within the Accelerating Medicines Partnership for AD (AMP-AD).[8] INPP5D deficiency has been shown to attenuate amyloid pathology in the 5xFAD mouse model of AD.[9] *INPP5D* encodes the Src homology 2 (SH2) domain–containing inositol polyphosphate 5-phosphatase 1 (SHIP1), a phosphatidylinositol phosphatase that regulates pathways downstream from TREM2[10,11] and the Fcγ receptor FCγRIIB.[11,12]

Triggering Receptor Expressed On Myeloid Cells 2 (TREM2) is a cell surface receptor expressed on immune cells. TREM2 plays a crucial role in modulating microglial response to neurotoxins and inflammation in the brain (Figure 1A). Hypomorphic variants of TREM2 have been associated with an increased risk of developing AD, and researchers have been exploring ways to activate TREM2 to potentially influence disease progression; however, results directly modulating TREM2 vary and the data are conflicting, depending on the model system used.[13,14] SHIP1 is a negative regulator downstream from TREM2. This complex, multidomain protein possesses a phosphatase (Ptase) domain flanked by a pleckstrin-homology (PH) domain that binds phosphatidylinositol (3,4,5)-trisphosphate [PI(3,4,5)P_3] and a C2 domain that binds phosphatidylinositol (3,4)-bisphosphate [PI(3,4)P_2] (Figure 1B).[15,16] The PH and C2 locate and orient the Ptase catalytic site toward its PI(3,4,5)P_3 substrate at the intracellular side of the membrane. The C2 domain is essential for cellular function, and interactions between Ptase and C2 modulate enzymatic activity.[17] SHIP1 converts PI(3,4,5)P_3 to PI(3,4)P_2, which are phosphorylated phosphatidylinositols that play important roles in membrane structure and identity and mediate downstream pathways such as AKT/mTOR signaling. For example, PI(3,4,5)P_3 binds and activates the PH-containing proteins PLCγ2, PDK1, and AKT.[18] SHIP1 also contains an N-terminal SH2 domain that binds immunoreceptor tyrosine-based inhibitory and immunoreceptor tyrosine-based activation motifs (ITIMs and ITAMs) on DAP12[10] and FCγRIIB[12,19] and a C-terminal proline-rich domain that binds many other proteins, including PLCγ2 and the Tec and Syk family kinases.[20] Therefore, SHIP1 is also involved in protein–protein interactions that modulate membrane structure and downstream signaling. Because SHIP1 binds receptor ITIMs and ITAMs, competes with kinases, and converts PI(3,4,5)P_3 to PI(3,4)P_2, it is generally understood as a negative regulator of cellular activation.[11] Although the role of SHIP1 in limiting microglial activation is not entirely understood, we hypothesize based on our previously reported human[21] and preclinical[9] results that inhibiting SHIP1 will increase the protective functions of microglia and reduce the rate of disease progression and cognitive decline in patients with AD. It is important to note that to investigate the biological function of SHIP1 and examine the consequences of its pharmacological manipulation, rigorously validated molecular tools are essential.[22] Therefore, we have characterized reported inhibitors, developed assays, screened for novel inhibitors, and evaluated the systemic and central exposure of a chemical probe in mice to further advance research in this area.

RESEARCH IN CONTEXT

1. **Systematic Review**: PubMed and SciFinder were searched to identify src homology 2 (SH2) domain-containing inositol phosphatase 1 (SHIP1) and SHIP2 inhibitors reported in the literature, and we screened for new inhibitors.
2. **Interpretation**: We evaluated the pharmacology of these inhibitors, assessed their suitability for animal studies, and discovered that not all reported inhibitors engage the target in cells and those that do drive different phenotypes in microglia like cell lines. One promising molecule activated microglia toward a phagocytotic phenotype, whereas others were cytotoxic. We characterized this molecule in primary mouse microglia and demonstrated that it can achieve micromolar exposures in brain tissue upon oral exposure in mice.
3. **Future Directions**: The work provides a molecular starting point for therapeutic lead discovery and assays for lead optimization. We also provide recommendations and cautions for the use of reported chemical probes that are used to explore the pharmacology of inhibitors of SHIP1.

2 | METHODS

2.1 | Ligand identification

The complex, multidomain, multifunctional nature of SHIP1, mediating multiple protein–protein interactions while serving as an interfacial enzyme at the intracellular side of the microglia membrane, motivated us to pursue multiple and orthogonal ligand identification strategies with the premise that engaging the target in multiple ways with different types of ligands would provide the array of molecular tools necessary to explore the pharmacology of SHIP1 inhibition.

We screened the SHIP1 Ptase domain,[23] analyzed a publicly available fragment-based screen,[24] and completed a thorough evaluation of SHIP1 and SHIP2 inhibitors reported in the literature.[25] Our screen using only the catalytic domain of SHIP1 was biased toward identifying orthosteric, active site inhibitors. Our analysis of the fragment-based screen[24] focused on compounds that bind in an allosteric site at the interface between the Ptase and C2 domains. Our literature evaluation focused on identifying starting points with drug-like properties and the synthesis of analogs to explore their potential for brain penetration. In each case, we prioritized chemical scaffolds that showed evidence of target engagement in cellular and in vivo biological contexts, with the expectation that ligands that engage the target differently would have different pharmacological activities depending on the biological context, timing, and the endpoints being evaluated.

2.2 | In vitro assay development

Once compounds were identified, they were evaluated in a series of SHIP1-related assays (Figure 1C). Due to the multidomain and multifunctional nature of SHIP1, we anticipated that discrepancies may arise between enzyme and cell assays, which could subsequently confound the interpretation of cellular results, as has been reported previously.[26,27] However, because enzyme activity is easily measured and provides evidence of target engagement, we elected to use the malachite green assay using PtdIns(3,4,5)P_3-diC8 as a substrate and a minimal enzyme construct containing the Ptase-C2 domains. This assay is standard in the field and is amenable to automated high-throughput screening.[28,29] The Ptase-C2 protein is well behaved, can be expressed and purified to a high degree of purity, and contains the allosteric site at the interface between the Ptase and C2 domains. For comparison and to assess potential species differences, inhibitors were tested against nearly full-length and stable SHIP1 protein constructs containing all ordered domains of the human and mouse proteins. We used a SHIP1 cellular thermal shift assay (CETSA) to provide evidence of target engagement in cellular assays. Because THP1 cells are employed frequently as a model of monocyte cells and SHIP1-dependent AKT signaling has been observed previously in this cellular context,[30,31] a signaling assay was established using THP1 cells measuring total AKT (tAKT) and phospho-Akt (pAKT) levels, which provides further evidence of on-target pharmacology. A phenotypic high-content imaging assay with simultaneous measures of phagocytosis, cell number, and nuclear intensity was used to ensure that the compounds are affecting desired cellular pharmacology without cytotoxicity.[32] Model cell lines, BV2 and HMC3, were used to provide adequate throughput for structure activity relationship (SAR) studies. Primary mouse microglia were used to ensure that observations in BV2 cells reflect primary cell activity.

2.3 | In vivo evaluation

To support therapeutic target validation studies of pharmacological SHIP1 inhibition in vivo, we selected a chemical probe with desired cellular pharmacology, analyzed its absorption, distribution, metabolism, and excretion (ADME) properties in silico, assessed key physicochemical and ADME properties in vitro, and utilized the results to predict plasma pharmacokinetics (PK) profiles. We then conducted a single-dose PK study to confirm that systemic peripheral and central exposures can be obtained in mice upon oral administration.

3 | RESULTS

As described in our Screening Target Enablement Resource,[23] 95K compounds were screened at 10 μM using the SHIP1 Ptase domain and produced three chemical series that were selected for further study (Figure 2A). The oxazyl pyrrole scaffold is represented by TAD-0058585 (**1**), the dihydrothienopyridine scaffold is represented by TAD-0058656 (**2**), and the tetrahydroquinoline scaffold is represented by TAD-0058581 (**3**). Because this screen was run using only the catalytic domain of SHIP1, these inhibitors are assumed to be orthosteric. Further elaboration and characterization of these scaffolds will be described elsewhere. Our analysis of the fragment-based screen by X-ray crystallography focused on reported compounds **4** (x-0524) and **8** (x-0101), which showed interpretable electron density in a binding pocket (Site 3) near Cys505 in the interface between the Ptase and C2 domains (Figure 2B). Studies with SHIP2 have demonstrated that the C2 domain is essential for cellular function, and its rigid interface with the Ptase domain enhances enzymatic activity.[17] Because the reported fragments did not inhibit SHIP1, we prepared analogs with improved activity. Adding a cyano group (**5**, **6**) to x-0524 proved effective, demonstrating increasing potency in the enzyme assay. The addition of 4-methyl benzoate (**7**) also improved enzyme inhibitory activity. Because this binding site contains a potentially reactive cysteine, we added the reactive functional group acryloyl to x-0101 to give compound **9**, which inhibited the enzyme, was active in CETSA, and yielded a crystal structure of the covalently modified protein (deposited in the Protein Data Bank [PDB 8UM5]). This structure is overlaid with the co-crystal structure of x-0101 and SHIP1 (PDB 5RWL)[33] in Figure 2B. These data provide evidence for binding in allosteric site 3 in the interface between the Ptase and C2 domains.

SHIP1 and SHIP2 inhibitors reported in the literature[25] are described in Figure 2C. Metabolically stabilized analogs of PtdIns(3,4,5)P_3, such as **10,** are stable, are not degraded by phosphatidylinositol phosphatases, and act as inhibitors[34]; however, they are neither selective for SHIP1 nor do they have the physicochemical properties required for studies beyond cellular assays. Likewise, phosphorylated polyphenols,[35] such as **11** and **12,** were deemed inadequate for our purposes because they are highly charged and are, therefore, unable to cross cell membranes. Consequently, we did not characterize these compounds. The aminosteroid **13,** known as 3α-aminocholestane (3AC), was first reported by the Kerr group[36] and is the most widely used SHIP1 inhibitor.[25,36–39] We also prepared and evaluated the more soluble aminosteroid analog K116 (**14**)[40,41] and several analogs of a tryptamine scaffold (**15-17**) reported by the Kerr group.[37] We obtained AS1949490 (**18**) and AS1938909 (**19**), a thiophene scaffold described by Astellas Pharma[42,43] as a

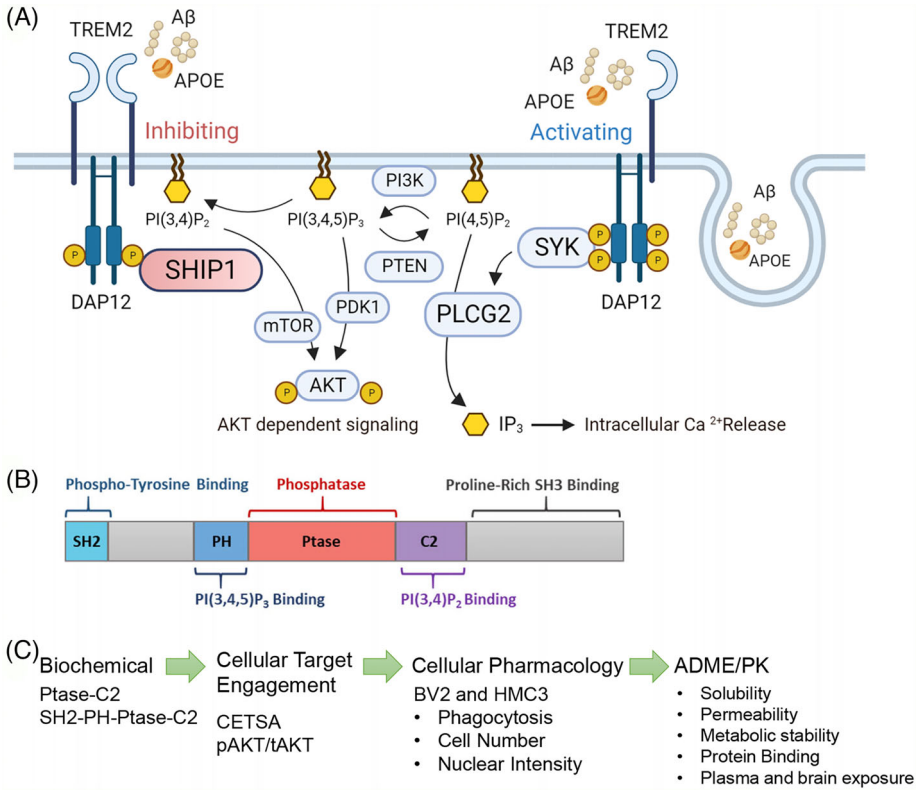

FIGURE 1 (A) Triggering Receptor Expressed On Myeloid Cells 2 (TREM2) binds amyloid beta (Aβ) and apolipoprotein E, which activate microgliosis and phagocytosis. DNAX activation protein of 12kDa (DAP12) mediates TREM2 activation through Spleen tyrosine kinase (SYK) and phosphatidyl inositol-specific phospholipase C-γ2 (PLCγ2). Src homology 2 (SH2) domain–containing inositol polyphosphate 5-phosphatase 1 (SHIP1) completes with SYK and modulates PIP3-dependent PLCγ2 and AKT signaling downstream from TREM2 by converting $PI(3,4,5)P_3$ to $PI(3,4)P_2$, both of which can activate AKT through PDK- and mTOR-dependent mechanisms depending on cell context. (B) Multi-domain structure of SHIP1 containing an N-terminal SH2 that binds immunoreceptor tyrosine-based inhibitory and immunoreceptor tyrosine-based activation motifs (ITIMs and ITAMs), a phosphatase (Ptase) domain flanked by a pleckstrin homology (PH) domain that binds $PI(3,4,5)P_3$, and a C2 domain that binds $PI(3,4)P_2$, and a disordered C-terminal end that binds many other proteins. (C) Flow of assays developed to assess SHIP1 inhibitors. The development of a cellular thermal shift assay (CETSA) to ensure cellular target engagement and a phenotypic assay with simultaneous measures of microglia activation (phagocytosis) and health (cell number and nuclear intensity) were critical for identifying compounds that engaged SHIP1 and resulted in desired pharmacology.

selective SHIP2 inhibitor with minimal activity against SHIP1. We also prepared NGD61181 (**20**), which was discovered by NeoGenesis Pharmaceuticals[44] using mass spectrometry-based affinity screening of a combinatorial library. Researchers at the University of Toyama noted similarities between the compounds reported by Astellas and NeoGenesis and used them as a starting point for a ligand-based design effort, culminating in the synthesis and evaluation of a pyridyl-based scaffold best represented by N-[4-(4-chlorobenzyloxy)pyridin-2-yl]−2-(2,6-difluorophenyl) acetamide (CPDA, **21**).[45] A similar pyridyl scaffold has been reported based on the observation that crizotinib, a multi-targeted kinase inhibitor, also inhibits SHIP2.[46] We prepared several analogs from this report, including compounds **22** and **23**.

3.1 | Evaluation of enzymatic inhibition

SHIP1 is an Mg^{2+}-dependent inositol 5'-phosphatase that converts $PI(3,4,5)P_3$ to $PI(3,4)P_2$ at the intracellular side of the cell membrane. Although our initial high-throughput screen relied on the Ptase-only catalytic domain, we used two-domain, $hSHIP1^{395-898}$ and $hSHIP2^{420-878}$, Ptase-C2 proteins for routine SAR studies of enzymatic inhibitory potency and selectivity because the C2 domain modulates the enzymatic activity of the Ptase,[17] and this protein contains both the catalytic site and a potential allosteric binding pocket at the interface between the domains. Using this protein allowed us to study both orthosteric and allosteric inhibitors. Although SHIP1 is an interfacial enzyme, we chose the soluble substrate PtdIns(3,4,5)P3-diC8. To account for the possibility that some inhibitors may have slow association rates, we preincubated compounds with the enzyme for 20 minutes before adding the substrate. We ran the reaction under initial velocity conditions, with the substrate concentration at the Km value to identify inhibitors (competitive, non-competitive, and uncompetitive). To minimize run-to-run variability, we also optimized the reaction to produce enough phosphate so that the malachite green reagent would provide sufficient signal-to-noise. Taking the initial rate and sufficient product for detection into account, we chose a 10-minute reaction time. The final reaction concentration of

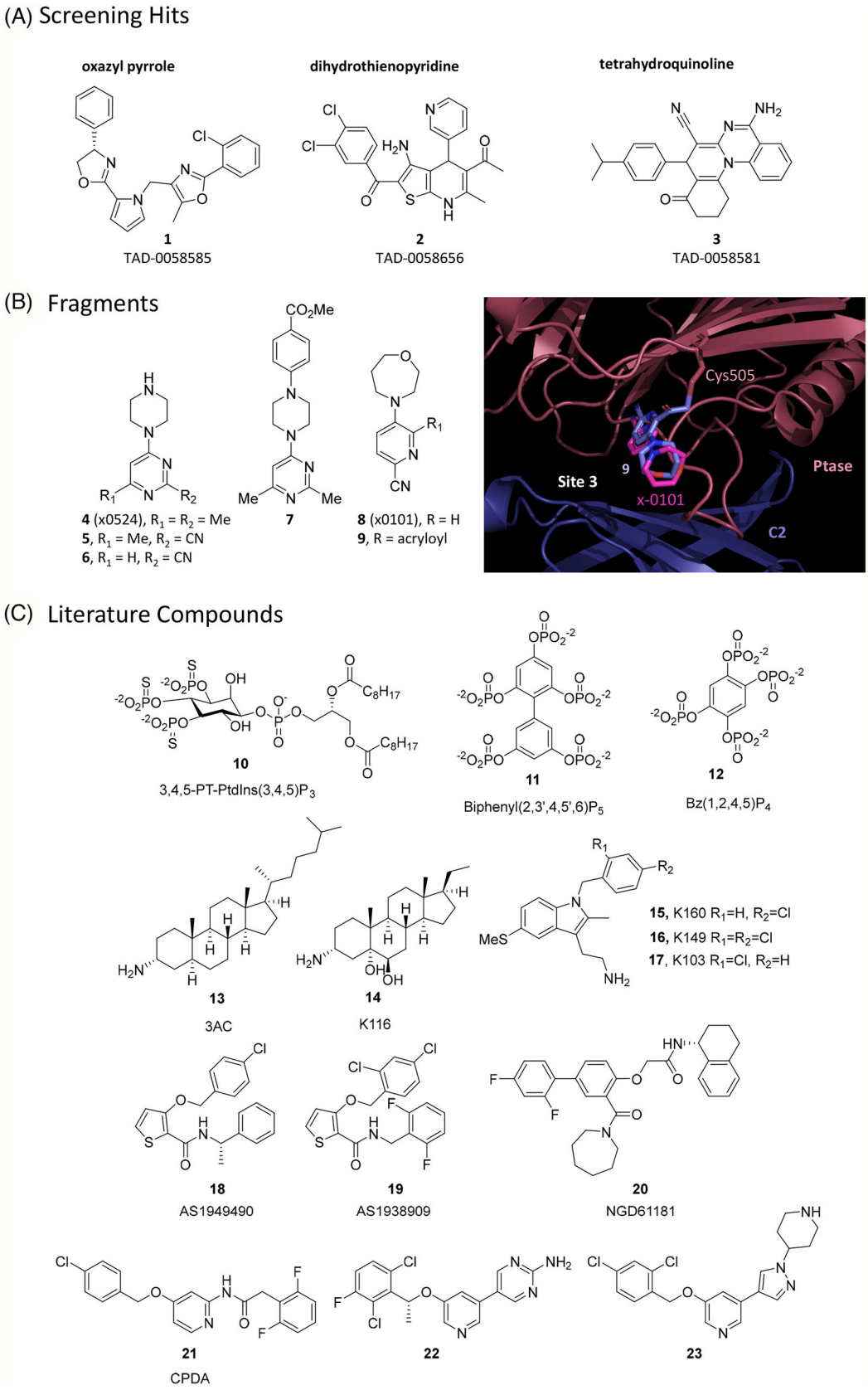

FIGURE 2 (A) SHIP1 Ptase domain inhibitors identified by high-throughput screening. (B) Fragment-based scaffold. Fragments **4** (x0524) and **8** (x0101) did not inhibit SHIP1. Adding cyano and 4-methyl benzoate groups to x0524 (5-7) increased enzyme potency and cellular target engagement. Compound **9** reacted with Cys505 and provided a crystal structure PDB 8UM5 (overlayed with PDB 5RWL). (C) SHIP1 inhibitors reported in the literature.

TABLE 1 Enzyme inhibition of the two-domain, hSHIP1$^{395\text{-}898,}$ and hSHIP2$^{420\text{-}878}$, Ptase-C2 proteins.

		human SHIP1 Ptase-C2					human SHIP2 Ptase-C2					
cmpd	Name	IC_{50} (μM)	SE	Upper (μM)	Lower (μM)	*N*	IC_{50} (μM)	SE	Upper (μM)	Lower (μM)	*N*	Selectivity
1	TAD-0058585	8.99	1.07	10.3	7.9	3	166	1.09	197	141	2	18.5
2	TAD-0058656	18.6	1.05	20.4	17.0	3	>300				2	>16
3	TAD-0058581	26.8	1.08	31.5	22.8	3	>900				2	>33
5		930	1.10	1119	773	2	1700				1	1.8
6		91.9	1.10	111	76.2	2	400				1	4.3
7		44.0	1.08	51.5	37.5	3	NT				0	
9		108	1.25	168	69.6	3	>800				1	>7
13	3AC	201	1.20	291	139	13	>900				4	>4
14	K116	122	1.26	193	77.3	8	151	1.54	358	64	4	1.2
15	K160	167	1.09	196	141	3	>500				3	>3
16	K149	49.1	1.09	58.4	41.3	7	128	1.21	188	87	4	2.6
17	K103	138	1.08	162	118	3	288	1.02	302	274	2	2.1
18	AS1949490	49.6	1.25	77.3	31.8	6	>900				4	>18
19	AS1938909	37.1	1.26	59.1	23.3	6	>900				4	>24
21	CPDA	31.9	1.09	38.1	26.8	6	>900				4	>28
22	Cmpd 43	79.4	1.13	102	62.0	15	>800				5	>10
23	Cmpd 10 h	251	1.13	321	197	6	252	1.06	281	225	4	1

SHIP1 and SHIP2 inhibitory potency values reported as the geometric mean of the inhibitory concentration at half maximum IC_{50} (μM) with the geometric standard error, multiplicative 95% confidence limits, and number of repeats (*N*).

the PI(3,4,5)P3-diC8 substrate was 52 μM, whereas the concentrations of the enzymes were 10 nM for SHIP1 and 50 nM for SHIP2. Reactions were quenched with Malachite BioMol Green and then incubated for 30 minute at room temperature and absorbance (620 nm) measured. Inhibitory potency at half maximum (IC_{50}) values were calculated by fitting absorbance versus inhibitor concentration and are reported in Table 1 for the compounds described earlier. Because full-length SHIP1 contains multiple folded domains and what is predicted to be a disordered C-terminal region, expression constructs containing the ordered domains were created to assess potential differences in activity compared to the two-domain Ptase-C2 protein. Furthermore, both human and mouse (hSHIP1$^{1\text{-}899}$ and mSHIP1$^{1\text{-}861}$) proteins were expressed, purified, and characterized to assess potential species differences. Enzymatic inhibitory potencies (IC_{50}) were determined for a subset of compounds as described earlier with the following changes: the reaction time was 2 minutes and the substrate concentration was 40 μM. The results are reported in Table **S1**.

3.2 | Demonstration of target engagement in cells

The multidomain and multifunctional nature of SHIP1 carries certain risks to lead optimization efforts; specifically differences between cell-free enzyme assays and cellular potencies can confound interpretation of SAR.[26,27] Therefore, we enabled a cellular target engagement assay to provide evidence that observed pharmacological activities were on target.[47,48] CETSA has become a routine assay to assess cell-based target engagement by quantifying changes in protein thermal stability upon ligand binding to endogenous proteins in intact cells.[49] A split Nano Luciferase (SplitLuc CETSA) version of the assay was used to provide sufficient throughput for SAR studies.[50,51] HMC3 cells were stably transfected with HiBit-INPP5D to express full-length human SHIP1 protein in a physiologically relevant cellular context. The thermal stability of this HiBit-labeled protein in intact cells was measured in two formats. In screening mode, cells were treated with a single concentration of compound (40 to 100 μM) or fragments (200 μM) at 37°C for 60 minutes and then exposed to 3-minute isothermal heating at 44.2°C, the experimentally determined melting temperature (Tm) of HiBit-SHIP1 ($n = 28$). In dose–response mode, cells were treated with decreasing concentrations from 100 μM (compounds) or 200 μM (fragments) with 1:3 serial dilutions to generate a percent of control 8-point curve. A half-maximum loss of luminesce (AC_{50}) was calculated using a four-parameter logistic curve regression model. Percent luminescence remaining at the highest concentration is also reported for the compounds when the difference from dimethyl sulfoxide (DMSO) vehicle control is greater than 3 times the standard deviation (SD). Otherwise, an AC_{50} was not calculated. Results are reported in Table 2 and example concentration–response curves for compounds **14** and **23** are shown in Figure S1.

TABLE 2 Cellular thermal shift assay (CETSA) and AKT signaling assay.

		CETSA			Signaling				
Cmpd	Name	AC_{50} (μM)[1]	%[2]	TE[3]	IC_{50} (μM)[4]	SE	Upper	Lower	*N*
1	TAD-0058585	NC	92	No	>60				1
2	TAD-0058656	46 ± 5 (2)	30 ± 7 (2)	Yes	12.4	1.36	22.98	6.72	2
3	TAD-0058581	173	63 ± 12 (2)	Yes	5.60	1.34	10.01	3.13	2
5		NT	NT	-					
6		NT	NT	-	>60				1
7		NC	77	No	>60				1
9		41	5	Yes	>60				1
13	3AC	NT	NT	-					
14	K116	97 ± 16 (4)	40 ± 20 (4)	Yes	2.93	1.12	3.7	2.3	1
15	K160	46	14	Yes	5.82	1.06	6.54	5.18	2
16	K149	NC	104	-	4.11	1.12	5.17	3.27	2
17	K103	89 ± 11 (2)	46 ± 21 (2)	Yes	4.59	1.14	6.00	3.52	2
18	AS1949490	NC	84	No	37.9				1
19	AS1938909	NC	75 ± 0 (2)	No	>60				1
21	CPDA	NC	92 ± 5 (2)	No	28.0				1
22	Cmpd 43	NC	92	No	5.85	1.14	7.58	4.52	2
23	Cmpd 10 h	54 ± 15 (3)	27 ± 15 (3)	Yes	6.52	1.03	7.06	6.16	2

[1]Concentration (μM) that induced a half-maximum loss of luminesce (AC_{50}) compared to control.
[2]Percent luminescence at the highest dose (100 μM).
[3]Target engagement was considered significant if change in melting temperature (ΔTm) difference from control at highest dose was >3SD, otherwise AC_{50} was not calculated (NC). NT = not tested.
[4]Reduction in the ratio pAKT/tAKT determined by Alpha SureFire assay and reported as the geometric mean of the inhibitory concentration at half maximum IC_{50} (μM) with the geometric standard error, multiplicative 95% confidence limits, and number of repeats (*N*) indicated.

3.3 | Cellular pharmacology

SHIP1 modulates AKT signaling because it converts $PI(3,4,5)P_3$ to $PI(3,4)P_2$ and both phosphatidylinositols bind and activate PH-containing proteins such as PDK1 and AKT.[11,18,52–54] Therefore, we established an AKT signaling assay in THP1 cells to provide further evidence of on-target activity. Cells were treated with inhibitors for 90 minutes and then the levels of phosphorylated and total AKT (pAKT/tAKT) were detected using the Perkin Elmer Alpha SureFire Ultra Multiplex PhosphoAKT (S473) kit. Results are reported in Table 2 and example concentration–response curves for compounds **14** and **23** are shown in **Figure S2**. Reduction in AKT phosphorylation was observed consistently in this cellular context when target engagement was confirmed by CETSA, except for compound **22**, a notable outlier that potently reduced pAKT but failed to destabilize the HiBit-SHIP1 protein.

Compounds that demonstrated significant cellular target engagement and changes in AKT signaling were evaluated in a phenotypic high-content imaging assay with simultaneous measures of phagocytosis, cell number, and nuclear intensity to assess both cellular pharmacology and cell health in parallel.[32] Model cell lines BV2 and HMC3 were used to provide adequate throughput. Microglia isolated from mouse brain were used to verify that results from the BV2 and HMC3 cells are mechanistically similar to those obtained with primary cells. Cells were treated with compounds for 24 hours and then seeded with pHrodo dye–labeled myelin. After 20 hours, nuclear staining solution was added, and the plates were incubated for another 30 minutes and then scanned with an ArrayScan XTI high-content analysis reader (Thermo Scientific), and the associated image data were analyzed with Thermo Scientific HCS Studio. Nuclei were stained with Hoetchst 33342 just before final high-content imaging scan. Because the assay is mix-and-read without liquid change, the imaging cell count is reliable. Mean total phagocytosis spot intensity per cell, total cell counts per well, and mean average nuclear intensity per cell for cell health were measured. Cellular potencies for each endpoint (EC_{50} for phagocytosis, IC_{50} for cell count) were calculated using a four-parameter logistic curve regression model. Results are described in Figure 3 and Tables **S2** and **S3**, and for compounds that demonstrated cellular target engagement as determined by CETSA.

Increased uptake of pHrodo-myelin, calculated as an effective concentration at half maximum (EC_{50}), is interpreted as a measure of microglial phagocytosis activation. Decreased cell count, calculated as an IC_{50}, is interpreted as decreased cellular proliferation and cell loss caused by mechanisms such as apoptosis. Cell counts are increased (calculated as an EC_{50}) or nuclear intensity is decreased (calculated as

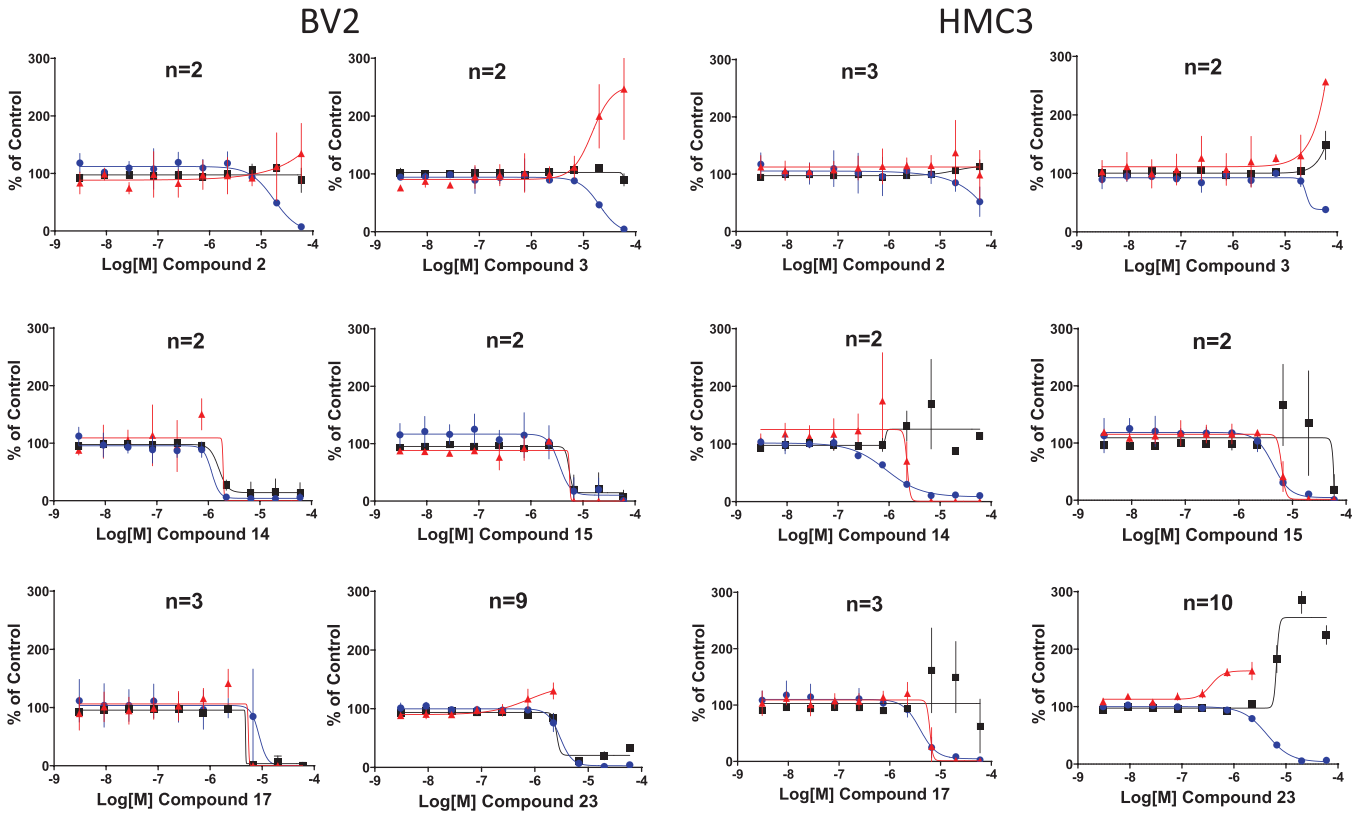

FIGURE 3 Effect of SHIP1 inhibitors on cell count (●), nuclear intensity (■), and phagocytosis (▲) in BV2 and HMC3 cells. *n* represents number of experiments.

an IC_{50}). The nature of these changes in cell count or nuclear intensity may be interpreted as early or late apoptosis, but further study such as TUNEL and caspase activation would be required to confirm. Compound **2** was inactive, demonstrating changes in BV2 and HMC3 cellular phenotypes only at the highest concentrations, consistent with high-dose cytotoxicity. Compound **3** increased phagocytosis at high concentrations probably due to cell stress; however, BV2 cell counts were reduced and early apoptosis may have been induced in HMC3 cells. Compound **14** may have caused late apoptosis of BV2 cells, as suggested by a reduction in cell count and nuclear intensity with an IC_{50} of 1 μM. In HMC3 cells, compound **14** decreased cell counts without increasing phagocytosis. The phenotype arising from treatment with compounds **15** and **17** was similar to that observed with compound **14**, although the effects of **17** were milder and are worth further investigation. Compound **23** consistently induced phagocytosis of both BV2 and HMC3 cells at concentrations that did not result in significant changes in either cell count or nuclear intensity. At high concentrations, cell counts were reduced and the compound appeared to induce late apoptosis (decreased nuclear intensity) in BV2 cells, but early apoptosis (increased nuclear intensity) was induced in HMC3 cells. Because compound **23** increased phagocytosis in the BV2 mouse microglial cell line 1.2- to 2-fold over baseline at concentrations of 1 to 2 μM with minimal effects on cell health, we tested its ability to activate primary mouse microglia isolated from neonate mice. Compound **23** increased phagocytosis 1.5-fold at concentrations that did not result in significant changes in either cell count or nuclear intensity up to 2.2 μM with a half maximal effective concentration (EC_{50}) of 540 nM (**Figure S3**).

3.4 | Pharmacokinetics

To assess the suitability of compound **23** for animal studies, in silico ADME properties were determined using Simulations Plus ADMET Predictor 10.2 software (Table S4). The reliability of ADMET Predictor to calculate these properties has been recently reviewed.[55] We then determined physicochemical and ADME properties in the following assays: kinetic solubility, microsomal stability intrinsic clearance (CL_{int}) in mouse liver microsomal solution, MDCK permeability (P_{app}), and protein binding (f_u) in mouse plasma and brain (Table S5). Plasma PK profiles were predicted using GastroPlus 9.8.2 from chemical structure and in vitro–derived plasma fraction unbound (f_u), NADPH-mediated clearance in mouse liver microsomes (CL_{int}), and MDCK permeability (P_{app}). Projected PK profiles for 10 and 100 mg/kg oral doses in mouse are shown in Figure 4 (dotted lines). We then conducted a single-dose pharmacokinetic (PK) study. The compound was formulated at 5 mg/mL in HPMC (1%)/Tween 80 (0.25%)/purified water. Male C57BL/6J mice, 8 to 12 weeks of age, from The Jackson Laboratory

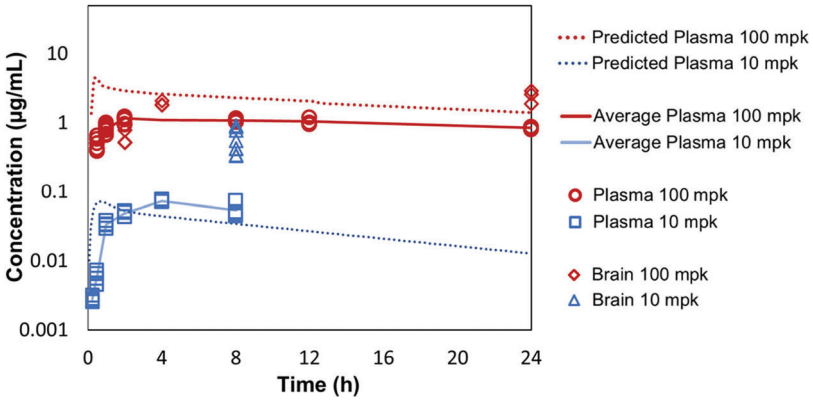

PK Parameter	10 mg/kg	100 mg/kg
Half-life (h)	30.0	44.4
Plasma C_{max} (µg/mL)	0.08	1.20
Plasma T_{max} (h)	4.00	2.00
AUC, 8 hrs (µg h/mL)	0.40	23.7
AUC, inf (µg h/mL)	3.00	78.2

FIGURE 4 **Pharmacokinetics.** Compound **23** demonstrated significant exposures in both plasma and brain with a brain/plasma ratio of 0.5- to 3-fold that increased over time.

(Jax #000664; *n* = 3–4) were dosed (10 and 100 mg/kg) via oral gavage (20 mL/kg). Plasma exposures were obtained at 0.5, 1, 2, 4, 8, and 12 hours and 24 hours. At the 10 mg/kg dose, brain exposures were determined at 8 hours. At the 100 mg/kg dose, brain exposures were obtained at terminal 2, 4, and 24 hours. Measured and average exposures (solid lines) are depicted in Figure 4 and corresponding PK parameters are reported.

4 | DISCUSSION

The goal of this work was to assess SHIP1 inhibitors with new assays and a novel strategy to ensure target engagement in cells and for animal studies. Figure 1C outlines the assays developed and Table S10 summarizes results for each compound in each assay. The differences observed between the SHIP1 Ptase-C2 and the human and mouse multi-domain forms of the protein demonstrate that the protein construct selected for enzyme assays is crucial and the lack of correlation with cellular potencies indicates that further studies are required to identify the best protein construct for biochemical assays. Given the complexity of the protein and difficulties translating a cell-free enzyme assay to cellular pharmacology, we executed a strategy using a combination of CETSA and target dependent signaling (pAKT) to provide evidence that cellular effects are mediated through SHIP1. The CETSA cellular target engagement assay provided crucial evidence that observed pharmacological activities were on target. Only about half of the compounds that inhibited the cell-free enzyme demonstrated significant cellular target engagement, consistently destabilizing the protein. Thermal stabilization of SHIP1 was not observed with any SHIP1 inhibitors. Compounds that did not appear to engage SHIP1 by CETSA were inactive in secondary cellular assays or simply cytotoxic at high concentrations. Although some SHIP1 inhibitors appeared to engage the target in cells, they did not activate phagocytosis and at high concentrations were cytotoxic. Other compounds increased phagocytosis only at high concentrations likely due to cell stress. Some compounds appeared to induce early or late apoptosis at lower concentrations. All SHIP1 inhibitors reduced the ratio of pAKT/tAKT in THP1 cells and this reduction was correlated to cytotoxicity in BV2 and HMC3, suggesting that reduced AKT signaling may be driving mechanisms of programmed cell death in these immortalized microglia-like cell lines. The reduced pAKT observed in THP1 cells is inconsistent with reports of increased AKT phosphorylation observed with SHIP1 inhibitors such as K116 in other cellular contexts.[41] The differences observed might indicate distinct signaling mechanisms through which $PI(3,4,5)P_3$ and $PI(3,4)P_2$ activate AKT signaling that are cell-context dependent.[56] Further studies with these compounds would be required to reconcile these differences in SHIP1-dependent AKT signaling.

Only compound **23** demonstrated target engagement by CETSA, reduced pAKT, and induced phagocytosis of both BV2 and HMC3 cells at concentrations that did not result in significant changes in either cell count or nuclear intensity. At high concentrations, compound **23** appeared to induce late apoptosis in BV2 cells and early apoptosis in HMC3 cells. Compound **23** also activated primary mouse microglia isolated from neonate mice. We cannot rule out that these effects may also involve other targets or mechanisms, but this compound was unique in its consistency across assays, lack of cytotoxicity, and favorable physicochemical and ADME properties. Therefore, we advanced it to studies with primary mouse microglia and in vivo PK studies in mice. Although compound **23** demonstrated significant exposures in both plasma and brain with a brain/plasma ratio of 0.5- to 3-fold, which increased over time, it should be noted that high protein binding (see Table S5) may limit its ability to sufficiently engage SHIP1 in vivo. Similar to other SHIP1 inhibitors we assessed, compound **23** exhibits potency in the micromolar range, a level somewhat greater than typically required for a clinical candidate in human studies. For most of the other SHIP1 inhibitors we evaluated, the combination of low potency and unfavorable chemical properties, such as poor solubility, creates significant challenges utilizing them as chemical probes for target validation. Compound **23** was unique in that its solubility and permeability, coupled with potency and relative lack of cytotoxicity, makes it a suitable lead-like molecule for a medicinal chemistry campaign to improve potency while maintaining drug-like properties. Therefore, SAR studies are being conducted by our team

around compound **23** to improve potency at SHIP1 to induce phagocytosis without cytotoxicity while increasing free-fraction exposures in vivo. These studies will be reported elsewhere.

ACKNOWLEDGMENTS

The logistical and project management support of Ariel Bontrager at Purdue University is gratefully acknowledged. The authors are grateful for the resources and support of the University of Pittsburgh Preclinical Phenotyping Core (PPC). Mass spectrometry was provided by the Clinical Pharmacology Analytical Core (CPAC) at Indiana University School of Medicine. The authors gratefully thank Louise Pay for editing the manuscript. This research was supported by the National Institute on Aging of the National Institutes of Health (NIH) under award U54 AG065181. KS was also supported by a Frederick N. Andrews graduate research fellowship. CPAC core facility was supported in part by the Indiana University Simon Cancer Center Cancer Center Support Grant P30 CA082709.

CONFLICT OF INTEREST STATEMENT

A.O., A.M., B.L., A.P., and T.R. are consultants for Monument Biosciences. B.L. receives licensing fees from Ionis Pharmaceuticals. He participates on the Advisory Board and receives consulting fees from NervGen Inc. and The Cleveland Clinic. He has a leadership or fiduciary role at the Alzheimer's Association and Cure Alzheimer's Fund. He has received travel support from Alzheimer's Association and Cure Alzheimer's Fund, and the United States Department of Defense. A.P. is president and Chief Executive Officer (CEO) of the Indiana Biosciences Research Institute. T.R. is an advisor for Enveda Biosciences. S.Q. received an honorarium from Thomas Jefferson University for a lecture. She participates on the Data Safety Monitoring Board for American Heart Association (AHA)–funded and National Institutes of Health (NIH)–funded studies relating to the effects of steroid hormones on QTc prolongation and drug–drug interactions between cannabidiol and tacrolimus. S.S.R. participates on the Data Safety Monitoring Board for the Alzheimer's Disease Cooperative Study, has received an honoraria for lectures from University of Wisconsin—Madison, Neumora Therapeutics, University of New Mexico, University of Texas San Antonio, and University of South Florida, and travel support from Rainwater Charitable Foundation and the Alzheimer's Association. C.J., G.D., P.H., D.B., S.S.R., and T.R. disclose that they have patents planned or pending. All funding provided to the institution and individual authors has been disclosed in the funding information and the declaration of interest section. No other authors have conflict of interests to disclose. Author disclosures are available in the Supporting Information.

CONSENT STATEMENT

No human subjects.

REFERENCES

1. Zhang B, Gaiteri C, Bodea LG, et al. Integrated systems approach identifies genetic nodes and networks in late-onset Alzheimer's disease. *Cell*. 2013;153(3):707-720. https://doi.org/10.1016/j.cell.2013.03.030
2. Jin SC, Benitez BA, Karch CM, et al. Coding variants in TREM2 increase risk for Alzheimer's disease. *Hum Mol Genet*. 2014;23(21):5838-5846. https://doi.org/10.1093/hmg/ddu277
3. Kierdorf K, Erny D, Goldmann T, et al. Microglia emerge from erythromyeloid precursors via Pu.1- and Irf8-dependent pathways. *Nat Neurosci*. 2013;16(3):273-280. https://doi.org/10.1038/nn.3318
4. Efthymiou AG, Goate AM. Late onset Alzheimer's disease genetics implicates microglial pathways in disease risk. *Mol Neurodegener*. 2017;12(1):43. https://doi.org/10.1186/s13024-017-0184-x
5. Target Enablement to Accelerate Therapy Development for Alzheimer's Disease. Accessed January 16, 2022, 2022. https://treatad.org/
6. Richardson T, Jesudason C, Chu S, et al. IUSM-Purdue TREAT-AD center target enabling component; INPP5D (SHIP1) chemical probe. *ZENODO*. 2022; https://doi.org/10.5281/zenodo.7231788
7. Lambert JC, Ibrahim-Verbaas CA, Harold D, et al. Meta-analysis of 74,046 individuals identifies 11 new susceptibility loci for Alzheimer's disease. *Nat Genet*. 2013;45(12):1452-1458. https://doi.org/10.1038/ng.2802
8. INPP5D inositol polyphosphate-5-phosphatase D Nominated Target. Accessed 12/30/2021, 2021. https://agora.adknowledgeportal.org/genes/(genes-router:gene-details/ENSG00000168918)
9. Lin PBC, Tsai APY, Soni D, et al. *INPP5D*deficiency attenuates amyloid pathology in a mouse model of Alzheimer's disease. *Alzheimer Dement*. 2022; https://doi.org/10.1002/alz.12849
10. Peng Q, Malhotra S, Torchia JA, Kerr WG, Coggeshall KM, Humphrey MB. TREM2- and DAP12-dependent activation of PI3K requires DAP10 and is inhibited by SHIP1. *Sci Signal*. 2010;3(122):ra38. https://doi.org/10.1126/scisignal.2000500
11. Pauls SD, Marshall AJ. Regulation of immune cell signaling by SHIP1: a phosphatase, scaffold protein, and potential therapeutic target. *Eur J Immunol*. 2017;47(6):932-945. https://doi.org/10.1002/eji.201646795
12. Ono M, Bolland S, Tempst P, Ravetch JV. Role of the inositol phosphatase SHIP in negative regulation of the immune system by the receptor Fc(gamma)RIIB. *Nature*. 1996;383(6597):263-266. https://doi.org/10.1038/383263a0
13. Gratuze M, Leyns CEG, Holtzman DM. New insights into the role of TREM2 in Alzheimer's disease. *Mol Neurodegener*. 2018;13(1):66. https://doi.org/10.1186/s13024-018-0298-9
14. Kulkarni B, Kumar D, Cruz-Martins N, Sellamuthu S. Role of TREM2 in Alzheimer's disease: a long road ahead. *Mol Neurobiol*. 2021;58(10):5239-5252. https://doi.org/10.1007/s12035-021-02477-9
15. Damen JE, Liu L, Rosten P, et al. The 145-kDa protein induced to associate with Shc by multiple cytokines is an inositol tetraphosphate and phosphatidylinositol 3,4,5-triphosphate 5-phosphatase. *Proc Natl Acad Sci U S A*. 1996;93(4):1689-1693. https://doi.org/10.1073/pnas.93.4.1689
16. Blunt MD, Ward SG. Pharmacological targeting of phosphoinositide lipid kinases and phosphatases in the immune system: success, disappointment, and new opportunities. *Front Immunol*. 2012;3:226. https://doi.org/10.3389/fimmu.2012.00226
17. Le Coq J, Camacho-Artacho M, Velazquez JV, et al. Structural basis for interdomain communication in SHIP2 providing high phosphatase activity. *Elife*. 2017;6, https://doi.org/10.7554/eLife.26640
18. Scheffzek K, Welti S. Pleckstrin homology (PH) like domains—versatile modules in protein-protein interaction platforms. *FEBS Lett*. 2012;586(17):2662-2673. https://doi.org/10.1016/j.febslet.2012.06.006
19. Ono M, Okada H, Bolland S, Yanagi S, Kurosaki T, Ravetch JV. Deletion of SHIP or SHP-1 reveals two distinct pathways for inhibitory signaling. *Cell*. 1997;90(2):293-301. https://doi.org/10.1016/s0092-8674(00)80337-2

20. Zhang J, Ravichandran KS, Garrison JC. A key role for the phosphorylation of Ser440 by the cyclic AMP-dependent protein kinase in regulating the activity of the Src homology 2 domain-containing Inositol 5'-phosphatase (SHIP1). *J Biol Chem*. 2010;285(45):34839-34849. https://doi.org/10.1074/jbc.M110.128827
21. Tsai AP, Lin PB, Dong C, et al. INPP5D expression is associated with risk for Alzheimer's disease and induced by plaque-associated microglia. *Neurobiol Dis*. 2021;153:105303. https://doi.org/10.1016/j.nbd.2021.105303
22. Bunnage ME, Chekler ELP, Jones LH. Target validation using chemical probes. *Nature Chem Biol*. 2013;9(4):195-199. https://doi.org/10.1038/nchembio.1197
23. Zhang Z-Y, Putt K, Chu S, et al. IUSM-Purdue TREAT-AD center target enablement resource; INPP5D (SHIP1) screening. *ZENODO*. 2022;https://doi.org/10.5281/zenodo.6208450
24. Bradshaw W, Priestley R, Obst J, Hall-Roberts H, Cederbalk A, Brennan P. SH2-containing-inositol-5-phosphatases (INPP5D); A Target Enabling Package. *ZENODO*. 2020;https://doi.org/10.5281/zenodo.4429248
25. Viernes DR, Choi LB, Kerr WG, Chisholm JD. Discovery and development of small molecule SHIP phosphatase modulators. *Med Res Rev*. 2014;34(4):795-824. https://doi.org/10.1002/med.21305
26. Schwaid AG, Cornella-Taracido I. Causes and significance of increased compound potency in cellular or physiological contexts. *J Med Chem*. 2018;61(5):1767-1773. https://doi.org/10.1021/acs.jmedchem.7b00762
27. Yu V, Pistillo J, Archibeque I, et al. Differential selectivity of JAK2 inhibitors in enzymatic and cellular settings. *Exp Hematol*. 2013;41(5):491-500. https://doi.org/10.1016/j.exphem.2013.01.005
28. Carter SG, Karl DW. Inorganic phosphate assay with malachite green: an improvement and evaluation. *J Biochem Biophys Methods*. 1982;7(1):7-13. https://doi.org/10.1016/0165-022x(82)90031-8
29. Pegan SD, Tian Y, Sershon V, Mesecar AD. A universal, fully automated high throughput screening assay for pyrophosphate and phosphate release from enzymatic reactions. *Comb Chem High Throughput Screen*. 2010;13(1):27-38. https://doi.org/10.2174/138620710790218203
30. Bosshart H, Heinzelmann M. THP-1 cells as a model for human monocytes. *Ann Transl Med*. 2016;4(21):438. https://doi.org/10.21037/atm.2016.08.53
31. Baran CP, Tridandapani S, Helgason CD, Humphries RK, Krystal G, Marsh CB. The inositol 5'-phosphatase SHIP-1 and the Src kinase Lyn negatively regulate macrophage colony-stimulating factor-induced Akt activity. *J Biol Chem*. 2003;278(40):38628-38636. https://doi.org/10.1074/jbc.M305021200
32. Mason ER, Soni DM, Chu S. Microglial phagocytosis/cell health high-content assay. *Curr Protoc*. 2023;3(3):e724. https://doi.org/10.1002/cpz1.724
33. Bradshaw WJ, Newman JA, Von Delft F, et al. INPP5D PanDDA analysis group deposition – Crystal Structure of the phosphatase and C2 domains of SHIP1 in complex with Z1348371854. *Protein Data Bank*. 2020; https://doi.org/10.2210/pdb5RWL/pdb
34. Zhang H, He J, Kutateladze TG, et al. 5-Stabilized phosphatidylinositol 3,4,5-trisphosphate analogues bind Grp1 PH, inhibit phosphoinositide phosphatases, and block neutrophil migration. *Chembiochem*. 2010;11(3):388-395. https://doi.org/10.1002/cbic.200900545
35. Vandeput F, Combettes L, Mills SJ, et al. Biphenyl 2,3',4,5',6-pentakisphosphate, a novel inositol polyphosphate surrogate, modulates Ca2+ responses in rat hepatocytes. *FASEB J*. 2007;21(7):1481-1491. https://doi.org/10.1096/fj.06-7691com
36. Brooks R, Fuhler GM, Iyer S, et al. SHIP1 inhibition increases immunoregulatory capacity and triggers apoptosis of hematopoietic cancer cells. *J Immunol*. 2010;184(7):3582-3589. https://doi.org/10.4049/jimmunol.0902844
37. Fuhler GM, Brooks R, Toms B, et al. Therapeutic potential of SH2 domain-containing inositol-5'-phosphatase 1 (SHIP1) and SHIP2 inhibition in cancer. *Mol Med*. 2012;18:65-75. https://doi.org/10.2119/molmed.2011.00178
38. Kerr WG, Pedicone C, Dormann S, Pacherille A, Chisholm JD. Small molecule targeting of SHIP1 and SHIP2. *Biochem Soc Trans*. 2020;48(1):291-300. https://doi.org/10.1042/BST20190775
39. Pedicone C, Meyer ST, Chisholm JD, Kerr WG. Targeting SHIP1 and SHIP2 in cancer. *Cancers (Basel)*. 2021;13(4)https://doi.org/10.3390/cancers13040890
40. Kerr W, Pedicone C, Chisolm JD, Dormann SM, inventors; Methods of Activating Microglial Cells. WO2020028552.
41. Pedicone C, Fernandes S, Dungan OM, et al. Pan-SHIP1/2 inhibitors promote microglia effector functions essential for CNS homeostasis. *J Cell Sci*. 2020;133(5); https://doi.org/10.1242/jcs.238030
42. Suwa A, Yamamoto T, Sawada A, et al. Discovery and functional characterization of a novel small molecule inhibitor of the intracellular phosphatase, SHIP2. *Br J Pharmacol*. 2009;158(3):879-887. https://doi.org/10.1111/j.1476-5381.2009.00358.x
43. Suwa A, Kurama T, Yamamoto T, Sawada A, Shimokawa T, Aramori I. Glucose metabolism activation by SHIP2 inhibitors via up-regulation of GLUT1 gene in L6 myotubes. *Eur J Pharmacol*. 2010;642(1-3):177-182.
44. Annis DA, Cheng CC, Chuang CC, et al. Inhibitors of the lipid phosphatase SHIP2 discovered by high-throughput affinity selection-mass spectrometry screening of combinatorial libraries. *Comb Chem High Throughput Screen*. 2009;12(8):760-771. https://doi.org/10.2174/138620709789104870
45. Ichihara Y, Fujimura R, Tsuneki H, et al. Rational design and synthesis of 4-substituted 2-pyridin-2-ylamides with inhibitory effects on SH2 domain-containing inositol 5'-phosphatase 2 (SHIP2). *Eur J Med Chem*. 2013;62:649-660. https://doi.org/10.1016/j.ejmech.2013.01.014
46. Lim JW, Kim SK, Choi SY, et al. Identification of crizotinib derivatives as potent SHIP2 inhibitors for the treatment of Alzheimer's disease. *Eur J Med Chem*. 2018;157:405-422. https://doi.org/10.1016/j.ejmech.2018.07.071
47. Seashore-Ludlow B, Axelsson H, Almqvist H, Dahlgren B, Jonsson M, Lundback T. Quantitative interpretation of intracellular drug binding and kinetics using the cellular thermal shift assay. *Biochemistry*. 2018;57(48):6715-6725. https://doi.org/10.1021/acs.biochem.8b01057
48. Robers MB, Friedman-Ohana R, Huber KVM, et al. Quantifying target occupancy of small molecules within living cells. *Annu Rev Biochem*. 2020;89:557-581. https://doi.org/10.1146/annurev-biochem-011420-092302
49. Tolvanen TA. Current advances in CETSA. *Front Mol Biosci*. 2022;9:866764. https://doi.org/10.3389/fmolb.2022.866764
50. Martinez NJ, Asawa RR, Cyr MG, et al. A widely-applicable high-throughput cellular thermal shift assay (CETSA) using split Nano Luciferase. *Sci Rep*. 2018;8(1):9472. https://doi.org/10.1038/s41598-018-27834-y
51. Oh-Hashi K, Furuta E, Fujimura K, Hirata Y. Application of a novel HiBiT peptide tag for monitoring ATF4 protein expression in Neuro2a cells. *Biochem Biophys Rep*. 2017;12:40-45. https://doi.org/10.1016/j.bbrep.2017.08.002
52. Singh N, Reyes-Ordonez A, Compagnone MA, et al. Redefining the specificity of phosphoinositide-binding by human PH domain-containing proteins. *Nat Commun*. 2021;12(1):4339. https://doi.org/10.1038/s41467-021-24639-y
53. Eramo MJ, Mitchell CA. Regulation of PtdIns(3,4,5)P3/Akt signalling by inositol polyphosphate 5-phosphatases. *Biochem Soc Trans*. 2016;44(1):240-252. https://doi.org/10.1042/BST20150214
54. Scheid MP, Huber M, Damen JE, et al. Phosphatidylinositol (3,4,5)P3 is essential but not sufficient for protein kinase B (PKB) activation; phosphatidylinositol (3,4)P2 is required for PKB phosphorylation at Ser-473: studies using cells from SH2-containing inositol-5-phosphatase

knockout mice. *J Biol Chem*. 2002;277(11):9027-9035. https://doi.org/10.1074/jbc.M106755200
55. Sohlenius-Sternbeck AK, Terelius Y. Evaluation of ADMET Predictor(TM) in early discovery DMPK project work. *Drug Metab Dispos*. 2021; https://doi.org/10.1124/dmd.121.000552
56. Manning BD, Toker A. AKT/PKB signaling: navigating the network. *Cell*. 2017;169(3):381-405. https://doi.org/10.1016/j.cell.2017.04.001

SUPPORTING INFORMATION

Additional supporting information can be found online in the Supporting Information section at the end of this article.

How to cite this article: Jesudason CD, Mason ER, Chu S, et al. SHIP1 therapeutic target enablement: Identification and evaluation of inhibitors for the treatment of late-onset Alzheimer's disease. *Alzheimer's Dement*. 2023;9:e12429. https://doi.org/10.1002/trc2.12429